Exploring life-long tissue homeostasis through lineage tracing and cell transplantation

Itai Rozenberg[1], Tehila Atlan[1], Roman Franek[1,2], Eitan Moses[1], Adi Oron-Gottesman[1], Henrik Chrzanowski[1], Itamar Harel[1,3]

1. Department of Genetics, the Silberman Institute, the Hebrew University of Jerusalem, Givat Ram, Jerusalem, 91904, Israel.
2. University of South Bohemia in Ceske Budejovice, South Bohemian Research Center of Aquaculture and Biodiversity of Hydrocenoses, Zatisi 728/II, 389 25 Vodnany, Czech Republic.
3. Corresponding author: itamarh@mail.huji.ac.il

Abstract:

Using lineage tracing and fate mapping strategies to study vertebrate aging has lagged behind developmental studies, primarily due to of the relatively long lifespans of classical models. Here, we introduce the *Killibow*, an inducible transgenic model for *in-vivo* multicolor lineage tracing in the naturally short-lived turquoise killifish (*N. furzeri*). We demonstrate that Cre-mediated recombination in transgenic fish can generate robust and stochastic labeling that remains stable during aging and regeneration. In addition, to achieve inducible control of recombination, we either utilize *in-vivo* Cre electroporation or use the tamoxifen system in *Killibow*-derived cells. To further enable transplantation assays, we establish the first immunocompromised killifish model by mutating *rag2*. RNA sequencing reveals that *rag2* mutants exhibit severely compromised expression of V(D)J recombination products, including immunoglobulins. Accordingly, we demonstrate that clearance of transplanted *Killibow*-derived cells is delayed in *rag2* recipients, and present a proof-of-principle for a $KRAS^{G12D}$ cancer model that is compatible with lineage tracing. Our platform provides the opportunity to examine tissue homeostasis, stem cell function, cancer dynamics, and tissue regeneration at unprecedented temporal resolution during vertebrate aging and disease.

Introduction:

Aging is accompanied by an increase in disease susceptibility and a decline in physiological functions[1–5]. Recent single-cell studies have advanced our understanding of the aging process, revealing complex variations in cell composition, identity, and lineage commitments[6–12]. However, single-cell transcriptomics as a tool is limited to distinct temporal snapshots, and therefore cannot be easily applied longitudinally. Thus, the question of how we can precisely track individual cells throughout organismal lifespan remains unanswered. Such results would allow us to link molecular identity with cellular lineages across vertebrate life-history.

Classical lineage tracing methods generally require stochastic and combinatorial labeling of individual cells *in-vivo*, either by employing spectrally distinct fluorescent proteins or genetic barcodes[13–16]. These approaches have greatly enhanced our understanding of many biological processes, including embryonic development, tissue regeneration, and tumor dynamics[17–19]. However, lineage tracing techniques in vertebrates have been primarily restricted to early life, because classical vertebrate models are relatively long-lived. Furthermore, while it has been suggested that the aging microenvironment itself can affect stem cell function[4], and tumor initiation and progression[19], the way in which lineage composition and commitments are modified during aging is largely unknown.

Many of these challenges can be addressed by the use of the turquoise killifish (*N. furzeri*) as a vertebrate model[20–25] (**Figure 1a**). With a naturally compressed lifespan of 4-6 months, killifish lifespan is 6-10 times shorter than that of mice or zebrafish, respectively. Thanks to the recently developed genomic and genome editing resources[23–30], these fish now provide an attractive experimental platform. To facilitate life-long lineage tracing, we first introduce the Cre/Lox system to the killifish model and develop the *Killibow*, a transgenic line that allows for stochastic and multispectral labelling of cells. Following Cre recombination, we can identify distinct lineages in either naïve animals or during regeneration. In particular, the system allows lineages to be investigated on the organismal, organ, and cellular levels.

To further enable functional interrogation of transplanted *Killibow* cells, we then describe the generation of an immunocompromised genetic killifish model. Specifically, we mutate the killifish *rag2* gene (*recombination activating gene 2*)[31–33], which is essential for generating the permutations of variable, diversity, and joining gene segments, commonly known as V(D)J[34]. RNA sequencing of the killifish head kidney (the equivalent of the mammalian bone marrow[35]), suggests that the expression of many V(D)J recombination

products, including immunoglobulins (Ig) and T-cell receptor genes, are severely compromised in *rag2* mutants. Finally, to explore cancer dynamics in aging, we establish a cell transplantation assay in *rag2* mutants, and generate an *in-vitro* tumor model by a stable overexpression of the human oncogenic $KRAS^{G12D}$ mutation (Kirsten Rat Sarcoma Viral Oncogene Homolog)[36–39]. Together, our platform represents a unique resource that enables rapid exploration of age-related functional changes in vertebrates, which could be instrumental for exploring stem cell function, cancer, and regeneration.

Results

Generation of an inducible *Killibow* transgenic line

To generate the *Killibow* transgenic line we used the *Zebrabow* construct[13], which was designed according to the strategy developed in mice[40]. The default expression of the construct is dTomato, a red fluorescent protein (RFP). Following Cre-mediated recombination, the expressed reporter is switched to either mCerulean, a cyan fluorescent protein (CFP), or EYFP, an enhanced yellow fluorescent protein (YFP, **Figure 1b**). This discrete expression, of either RFP, CFP, or YFP, is made possible by two pairs of Lox sites, LoxP and Lox2272, which are mutually incompatible. Thus, recombination is irreversible, and can occur only once (**Figure 1b**, left). Reporter expression is controlled by the zebrafish ubiquitin promoter[41], which allows for a ubiquitous and continuous expression. Importantly, the ubiquitin promoter was previously shown to be expressed in a broader range of cell types than other commonly used promoters such as the β-actin-2[13,42].

Tol2-based transgenesis was performed in fertilized killifish eggs as previously described[23,27], and a founder transgenic line with high and uniform expression was selected. Using standard qPCR approaches[13] we were able to estimate that the number of transgenic insertions in the *Killibow* line is ~70 (see **Methods**). In the absence of Cre recombination, the *Killibow* line fish exclusively express RFP (**Figure 1b**, right). While expression is very weak during early development (i.e. early somitogenesis, ~7 days post fertilization, **Figure S1a**), it increases rapidly when entering organogenesis, and persists throughout adulthood (**Figure 1b**, right). These findings are a characteristic of the ubiquitin promoter, and are conserved in zebrafish[13].

Cre mRNA induces a dose-dependent and heritable multicolor stochastic labeling

To test whether Cre-mediated recombination could produce broad multicolor labeling, we microinjected Cre mRNA into one- or two-cell stage *Killibow* embryos (**Figure 2a**, left). High

Cre mRNA concentrations (~20 ng/µg) produced fish that express only a blue-green color combination, probably due to saturation of recombination events (**Figure S2a**). However, at lower mRNA concentration (~5 ng/µg), we were able to obtain multicolor labeling throughout the killifish body with relatively large clones, as a result of recombination in early development (**Figure 2a**, right). These clones could easily be detected in internal organs, including the liver, intestine, and testis (**Figure 2b**).

Crossing Cre-injected adult *Killibow* fish with WT fish produced offspring that were uniformly colored in a variety of hues (**Figure 2c**), indicating efficient labeling of the killifish germline. Finally, we utilized our recently-developed *in-vivo* electroporation system[43] to induce Cre-mediated recombination at will (**Figure 2d**, left). Specifically, we electroporated a Cre-GFP plasmid following intramuscular injection. As it is difficult to distinguish between plasmid-encoded GFP and the YFP in the *Killibow* construct, only the emergence of CFP was used to assess successful recombination (**Figure 2d**, right). These results demonstrate that Cre-mediated recombination is an efficient method of generating stochastic and stable labeling in killifish.

Tail-fin regeneration in old *Killibow* transgenic fish

A decline in regenerative potential is a classical hallmark of aging[44,45]. Exploring this functional decline using lineage tracing could provide the means to uncouple autonomous (e.g. stem cell number or function) from nonautonomous mechanisms (e.g. the immune system). We chose tail-fin regeneration[45] as an experimental platform to examine whether the color combinations are stable throughout organismal lifespan and following tissue damage. Specifically, we examined regeneration by monitoring regrowth of the tail fin after dissection[45] (**Figure 3a**), in young (1-month old) and old (4.5-month old) transgenic fish, which were injected with Cre mRNA as single-cell embryos ($n > 4$, **Figure 3b**). A global view suggested that lineage commitments are largely stable during tissue regeneration, and are comparable between young and old fish. Our findings to date suggest that the *Killibow* transgenic model produces robust and stable expression across organismal lifespan, and can therefore be used as a reliable tool for lineage tracing during vertebrate aging.

Exploring Cre activation in a *Killibow*-derived stable cell-line

Next, as the first step in developing a method for transplanting *Killibow*-derived cells, we isolated tail-fin fibroblasts[46] from the *Killibow* transgenic fish (**Figure 4a**). Continuous propagation (~20 passages) resulted in spontaneous immortalization, and we obtained a stable

cell-line that expresses RFP in a robust and uniform manner (**Figure 4b**). We then modified our recently developed doxycycline-inducible system in killifish[43] to induce Cre recombination at will. To this end we tested two plasmids that use the tamoxifen-inducible Cre system[47,48], namely the pCAG-ERT2-Cre-ERT2 plasmid (Addgene #13777), and the Tol2-ubi-ERT2-Cre-ERT2 plasmid (a kind gift from Wang Wei).

Transfection and tamoxifen treatment in *Killibow*-derived cells (see **Methods**) produced inducible and dose-dependent multicolor stochastic labeling (**Figures 4b, S4a**). The appearance of uniformly-colored clones suggests that the color combinations are stable in the daughter cells in culture. Furthermore, the Tol2-based plasmid could ultimately be used for stable transgenic integration in both cells and fish. This opens the possibility of transplantation studies. However, no immunodeficient killifish model has yet been developed.

Generation and characterization of a *rag2* genetic model

To generate an immunodeficient killifish model, we mutated the *rag2* gene (**Figure 5a**). *Rag2* is a core member of the multiprotein RAG complex. This complex is responsible for generating the diverse repertoire of immunoglobulins and T-cell receptor genes through permutations of V(D)J rearrangements (recently studied in killifish[34]). Here we used our previously developed CRISPR protocol[23] to generate a ~250 base-pair deletion (Δ250) allele in the single exon in the killifish *rag2* coding sequence (**Figure 5a**). We then outcrossed this line for several generations and succeeded in generating viable and fertile homozygous fish.

Murine *rag2* mutants display hematopoietic and immune system defects, including arrested B-cell and T-cell development[49]. We therefore compared the transcriptome of the killifish head kidney, the equivalent of the mammalian bone marrow (see **Figure 2b**, left), from three wild-type and three *rag2* mutants. Principle component analysis (PCA) demonstrated that certain samples segregate according to genotype (PC3, **Figure 5b**). The differential expression analysis revealed 103 downregulated and 68 upregulated genes, with a FC > 2 and a p-value of 0.05 (uncorrected, **Figure 5c, Table S1**). As the next step, we conducted gene ontology (GO) enrichment analysis on the up- or down-regulated genes. The results confirmed an enrichment of downregulated adaptive immunity-related pathways (including B-cell activation, and T-cell selection), and an upregulation of pathways associated with innate immune responses (e.g. type I interferon signaling, **Figure 5d, Table S1**).

The majority of the downregulated genes are directly related to *rag2* functions, including members of the immunoglobulin light chain-related genes (e.g. *Igkv4-1*) and the T-

cell receptor complex (e.g. *cd3d*) (**Figure 5c**). We therefore plotted the precise fold change of primary T-cell receptor and immunoglobulin genes, which are significantly compromised in the *rag2* mutants (**Figure 5e**, left). These data suggest that failure to rearrange the V(D)J gene segments results in loss of expression, and that the *rag2* killifish mutants probably lack functional features of B-cell and T-cells.

In contrast, we identified upregulation of several gene families in the *rag2* mutants, including the novel immune-type receptors (NITRs)[50–55], such as *nitr9* and *nitr13* (**Figure 5e**, right). NITRs have been identified in all major lineages of teleost fish[56], and are structurally similar to the killer immunoglobulin-like receptors (KIR) on mammalian natural killer (NK) cells[54]. The receptors typically encode two extracellular Ig domains, which do not depend on V(D)J recombination[56], and are expressed in teleost NK-like cells[54,57]. NK cells play an important role in recognizing "non-self", and therefore in the defense against infection and malignancy. Interestingly, expansion of NK-like cells was previously detected in zebrafish *rag2* mutants[53], suggesting an evolutionary conserved compensatory mechanisms of the innate immune system in bony fishes.

Developing transplantation assays for exploring cancer lineage composition

Next, we developed a proof-of-principle cancer model in *Killibow*-derived cells by overexpressing a human oncogenic KRAS mutation[36–39] (Kirsten rat sarcoma viral oncogene Homolog), the $kras^{G12D}$, in *Killibow*-derived cells. Specifically, we synthesized the human $kras^{G12D}$ mutation using gene blocks synthesis (IDT), and then used Gibson assembly to clone it into a lentiviral expression vector (**Figure S5a**). Lentiviruses were produced using standard protocols, and used to transduce *Killibow*-derived cells. As the lentiviral vector also delivers a hygromycin antibiotic resistance, cells were grown under selection to generate a stable cell-line, which can be used to study cancer models in killifish.

Finally, the naïve *Killibow* cell-line was used to develop a transplantation assay (**Figure 4a**), which involves injecting WT or *rag2* mutant fish intramuscularly with ~160,000 cells per fish (**Figure 5f**, top). The fish were monitored for 5 days following injection, and red fluorescence was imaged at the same exposure parameters. Our findings suggest that on average, clearance of injected cells was 50% faster in WT controls compared to *rag2* mutants (2 vs. 3 days, respectively. n≥5 for each experimental conditions). In extreme cases, cells were visible even until day 5 in *rag2* mutants (**Figure 5f**, bottom). In conclusion, our unique set of tools combine multispectral lineage tracing, an immunodeficient killifish model, and a method

for cellular transplantation. This platform represents a comprehensive approach for exploring tissue homeostasis during vertebrate aging at an unprecedented temporal resolution.

Discussion:

As the most diverse group of vertebrates, fish species exhibit a vast range of evolutionary adaptations, providing an experimental playground for modeling complex traits in health and disease[58–62]. Here, using the naturally short-lived turquoise killifish, we describe a comprehensive platform for exploring life-long lineage tracing, tissue homeostasis, cell transplantation, and regeneration during vertebrate aging. The strength of the multicolor *in-vivo* labeling is demonstrated by the *Killibow* transgenic line, in which color combinations are faithfully inherited between daughter cells and are stable over time. This model also introduces the Cre/Lox system to the killifish model, and should stimulate the killifish community to generate tissue-specific and inducible Cre drivers. We further enhance possible experimental applications by developing the *rag2* immunodeficient model, which is compatible with transplantation studies.

Dissecting the molecular mechanisms that regulate tissue homeostasis and regeneration is vital for understanding degenerative processes[1–4]. Following cells and their progeny, using either lineage tracing or fate mapping strategies[16], could be instrumental for this purpose. Lineage tracing attempts to identify the progeny of an individual cell, to ultimately reconstruct lineage relationships. This approach could be applied to identify whether senescent cells within a tissue are more likely to originate from a limited number of tissue-resident stem cells, or are a random event with equal probability. In contrast, fate mapping is classically used to identify which part of an embryo contributes to which adult tissue (or cell type). Fate maps can provide spatial information, which is often lost in lineage hierarchies. This methodology could be used to assess whether tissue homeostasis is altered with age, by monitoring the borders between different clones, overall clonal heterogeneity, and their relative size over time.

Similar to the role of stem cells in normal tissue homeostasis, tumor growth can also be modified by cancer stem cells[17–19]. While lineage-tracing techniques have provided insights into tumor dynamics (e.g. the therapeutic response of cancer stem cells[63]), the way in which tumor lineage composition is modified by the aging microenvironment remains largely unknown[19]. The *rag2* genetic model we have developed can serve as a universal recipient for cell transplantation into old fish. This tool could introduce a new era for exploring how the aging niche affects classical processes, including stem cell self-renewal and the clonal

heterogeneity of cancer and metastasis. Together, we add to the continently expanding toolkit for the killifish model system[64–67], by providing a transformative resource for advanced color-based anatomical and lineage analyses during vertebrate aging and disease.

Figure 1

a. The turquoise killifish, a naturally short-lived vertebrate with a compressed lifespan

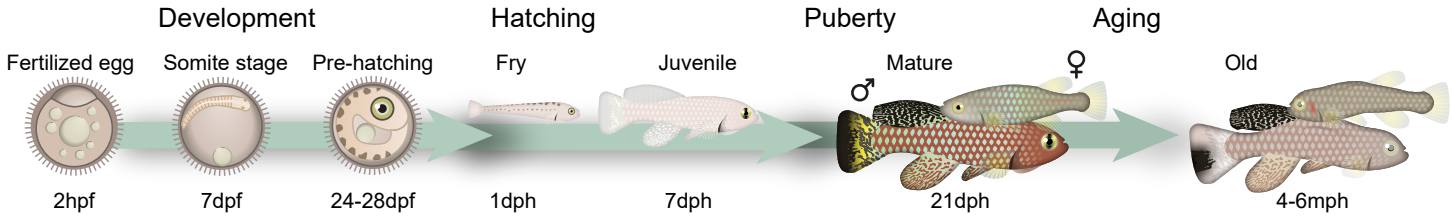

b. Generation of the *Killibow* transgenic line

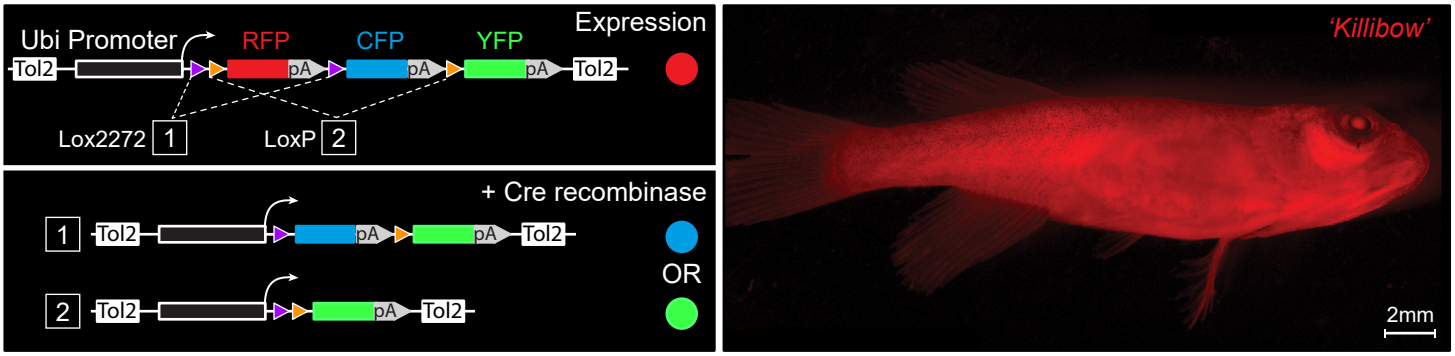

Figure S1

a. Killibow expression in early embryonic development

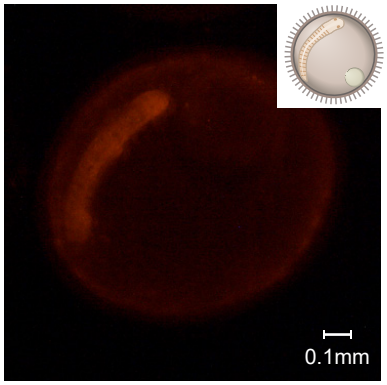

Figure legends:

Figure 1: Generation of the *Killibow* transgenic line

a) The life history of the turquoise killifish *N. furzeri*, including primary stages and accompanying timelines. Fish reach sexual maturity after 2-3 weeks, and display typical signs of vertebrate aging after a few months. dpf, days post-fertilization; dph, days post hatching; mph, months post hatching.

b) The *Zebrabow* construct[13] (left) was used to generate the *Killibow* transgenic line (right). The Cre recombinase can recognize either Lox2272 (purple arrowheads) or LoxP (orange arrowheads) sites, resulting in excision of sequences flanked by the Lox sites. Because Lox2272 and LoxP are mutually incompatible, recombination occurs only between identical Lox sites (event 1 or 2). Expression is determined by whether/which recombination event occurs.

Figure S1: Reporter expression in the *Killibow* during embryonic development

a) The *Killibow* transgenic line starts to express fluorescent proteins during mid development.

Figure 2

a. Stochastic multicolor labeling following Cre mRNA injection

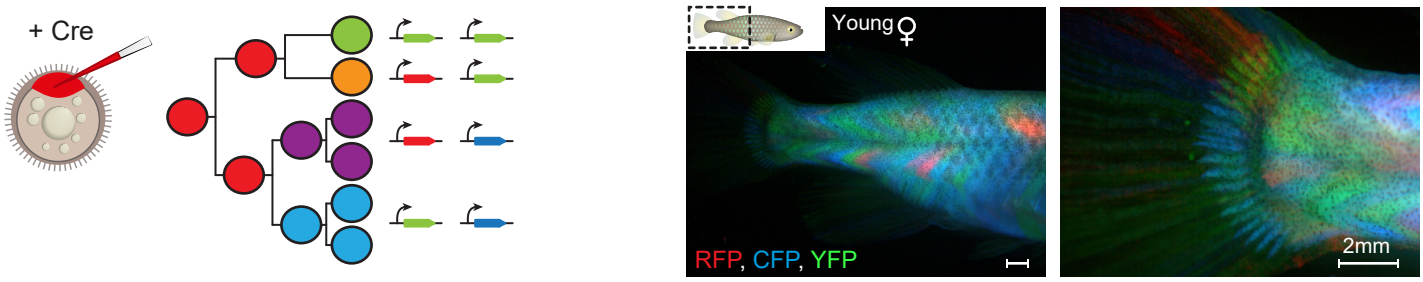

b. Labeling of internal organs

c. Successful germline recombination following Cre mRNA injection

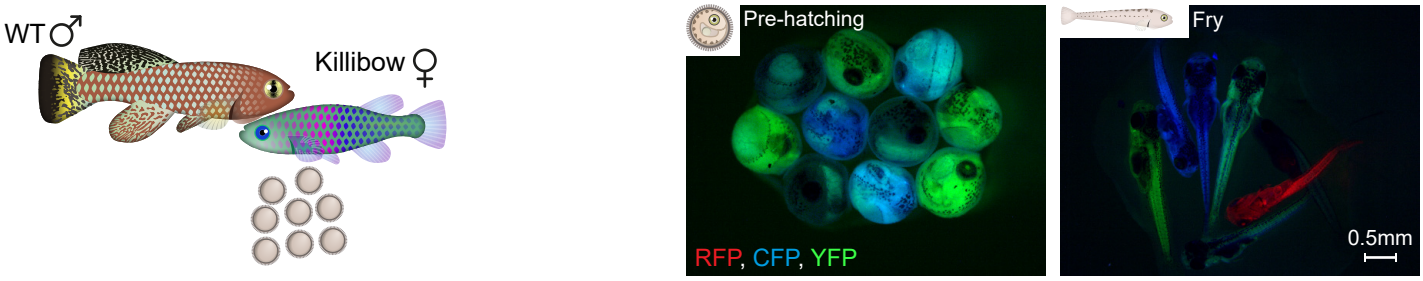

d. A plasmid electroporation system for inducible Cre-mediated recombination

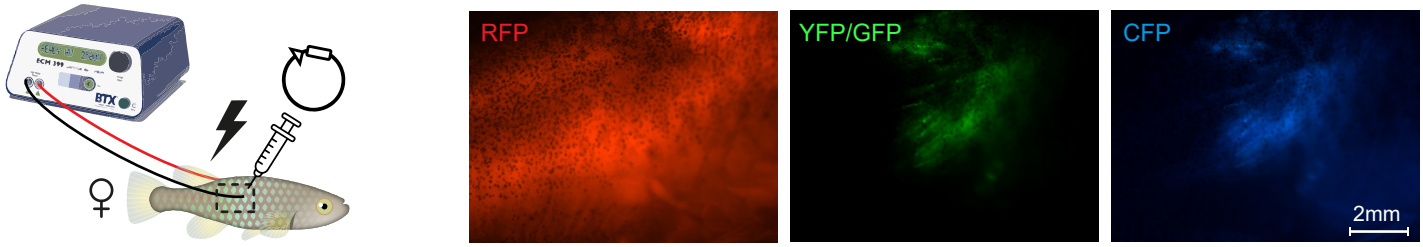

Figure S2

a. Multicolor labeling following saturated Cre-mediated recombination

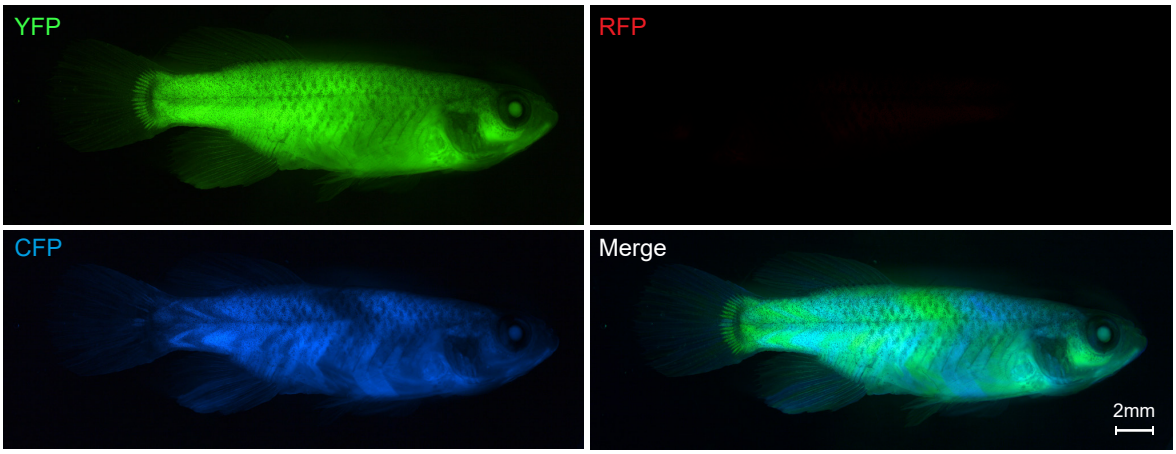

Figure 2: Cre-mediated multicolor labeling is stable in internal organs and across generations

a) Following the injection of Cre mRNA into fertilized *Killibow* eggs (left), stochastic multicolor labeling is visible in the trunk and tail fin of adult fish (right).

b) Dissection of selected organs in Cre-injected fish demonstrates widespread labeling.

c) Mating Cre-injected fish with WT fish produces a variety of single colored offspring, demonstrating uniform and stable germline transmission. $n \geq 4$ for all experimental conditions.

d) Left: Schematic illustration of the intramuscular plasmid electroporation approach. Right: Because GFP cannot be easily distinguished from transgenic YFP following the electroporation of the Cre-GFP plasmid, only CFP is used to validate recombination ($n = 4$).

Figure S2: Cre-mediated recombination is saturated at high mRNA concentrations

a) Injection of large amounts of Cre mRNA saturates recombination to the point that the red color is no longer visible.

Figure 3

a. Experimental design

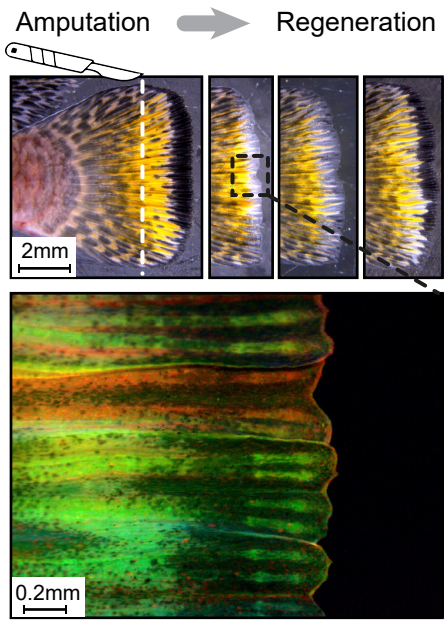

b. Age-related regeneration dynamics

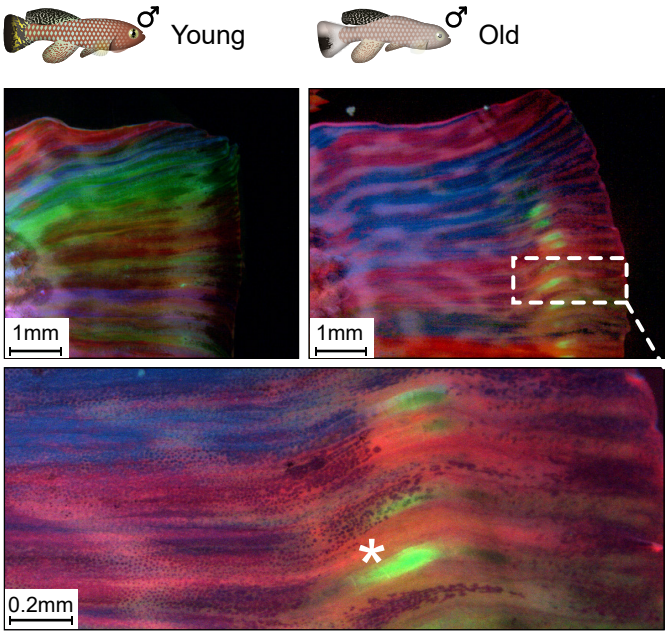

Figure 3: Lineage tracing during tail-fin regeneration in young and old fish

a) Top: experimental workflow for assessing tail-fin regeneration. Following tail fin amputation, regrowth was measured every three days for a total of 18 days. The white dashed line represents the amputation plane. Bottom: enlarged view of the area marked by a dashed rectangle, showing an example of partial tail fin regeneration at 6 days after amputation.

b) Examples of regenerated tails at day 18 post amputation, in young (top left) or old (top right) male Cre-injected *Killibow* fish. Bottom: enlarged view of the area marked by a dashed rectangle, showing the range of possible colors. Green autofluorescence from regenerating bones is marked by an asterix. $n \geq 4$ for all experimental conditions. Scale bars are indicated.

Figure 4

a. Generation of fibroblast cell line from the *Killibow* transgenic line

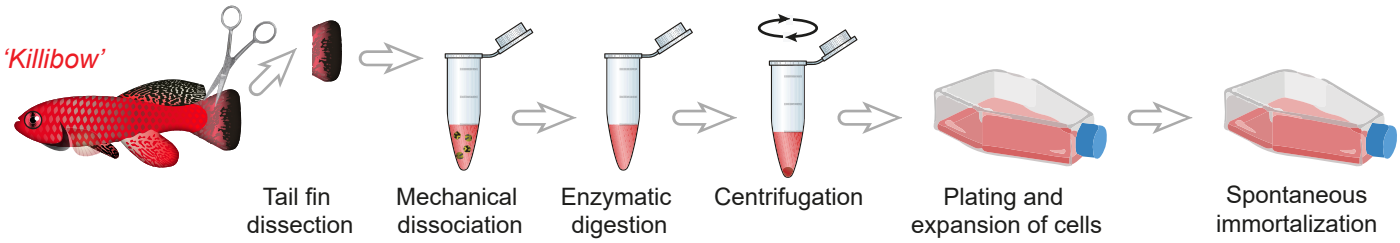

b. Induction of multicolor stochastic labeling in cultured fish cells

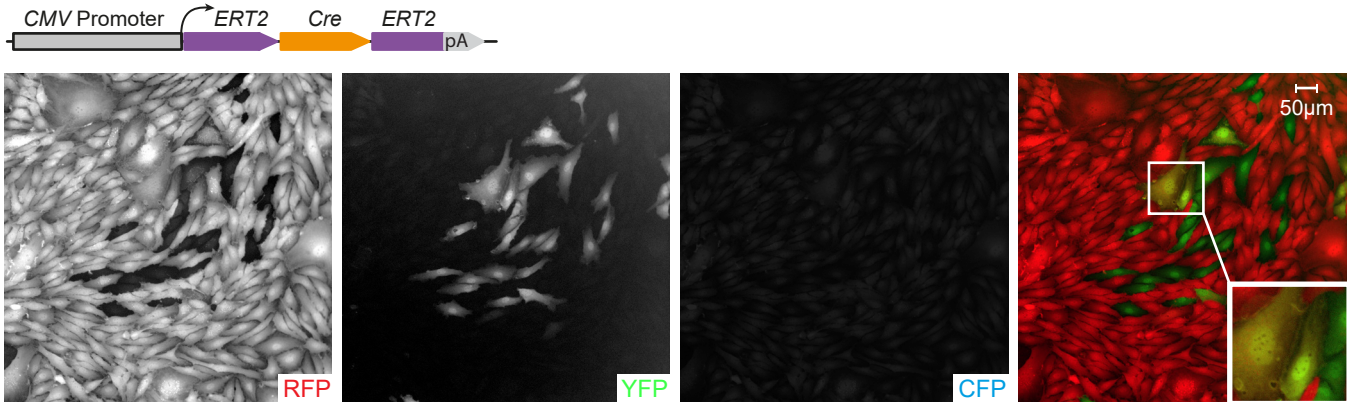

Figure S4

a. Induction of multicolor stochastic labeling in cultured fish cells

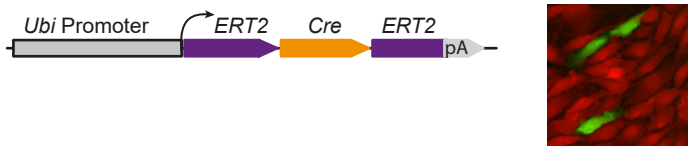

Figure 4: Stable multicolor clones of cultured *Killibow* fibroblasts are obtained by using a tamoxifen-inducible Cre

a) Schematic illustration depicting the isolation procedure of primary fibroblasts from the tail-fin of a *Killibow* male fish.

b) Clonal analyses of cultured *Killibow* cells. Cre-mediated recombination was induced by the transfection of an ERT2-Cre-ERT2 plasmid, followed by tamoxifen treatment.

Figure S4: Cre-mediated recombination using a Tol-based plasmid in cultured cells

a) A Tol2-ubi-ERT2-Cre-ERT2 plasmid can successfully induce recombination in cultured *Killibow* cells, following transfection and tamoxifen treatment.

Figure 5

a. Generation of *rag2* CRISPR mutants

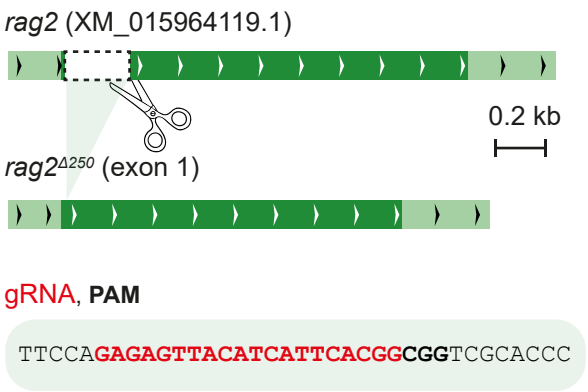

b. PCA for transcript levels in the head kidney of WT and *rag2* mutants

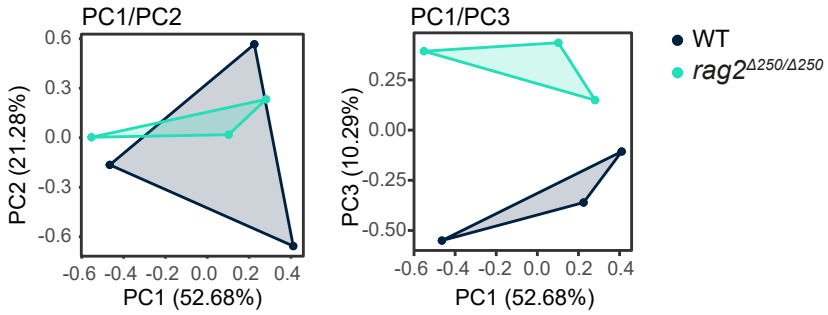

c. Volcano plot highlights the involvement of immune related genes

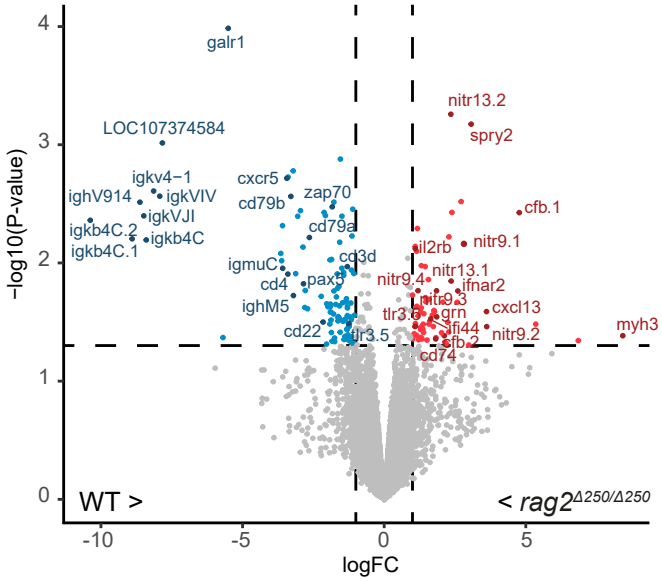

d. GO enrichment analysis

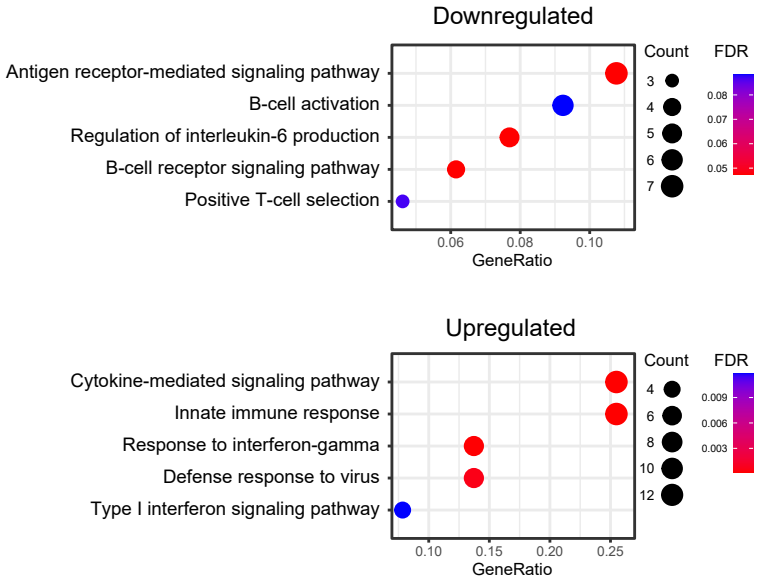

e. Barplot of selected up- and down-regulated genes

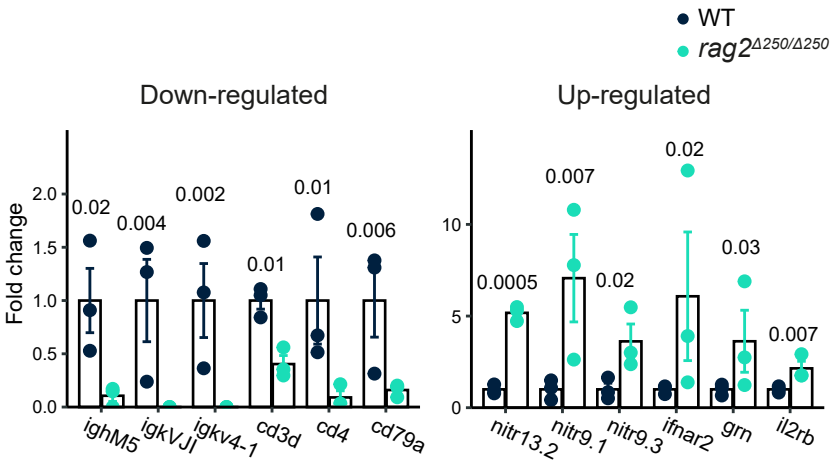

f. Clearance of injected *Killibow* cells

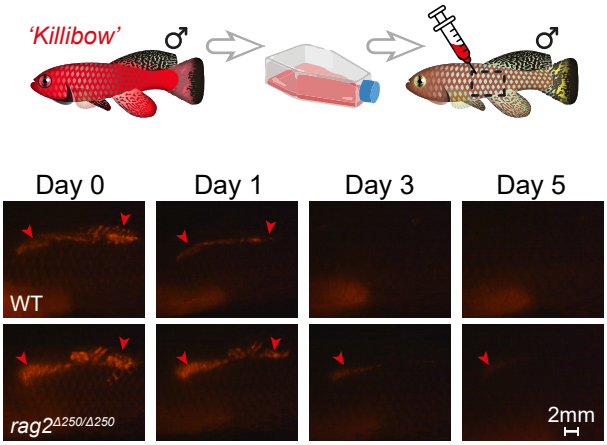

Figure S5

a. *KRAS*^{G12D} transgenic plasmid

Figure 5: Generation of an immunodeficient model by mutating the killifish rag2

a) Generation of a *rag2* CRISPR mutant with a ~250 bp deletion (Δ250). Gene model with a single exon is shown. Guide RNA (gRNA) targets are in red, protospacer adjacent motif (or PAM) in bold.

b) PCA for transcript levels from the head kidney of WT (black) and *rag2* mutant fish (green). Each symbol represents an individual fish. PC1, 2, and 3 are presented.

c) Volcano-plot presenting the differential gene expression between WT and *rag2* mutant fish. The dashed lines represent the statistical threshold for the GO analysis. Upregulated genes are in shades of red, and downregulated genes in shades of blue. The various shades are used to facilitate the distinction of datapoints with an associated gene name.

d) Functional enrichments (GO) for differential gene expression between WT and *rag2* mutant fish (p-value < 0.05, and FC > 2). Distinct genotype profiles are observed. GO enrichments were called at FDR < 5%.

e) Bar-plot of selected genes normalized to the WT; either down (left) or up (right) regulated genes. Error bars represent mean ± SEM. Significance was called as part of the edgeR pipeline.

f) Representative images following the injection of the *Killibow*-derived cell-line into either WT (top) or *rag2* mutant fish (bottom). Equal numbers of cells were injected, and fish were imaged at the indicated days. n = 4 for each experimental group.

Figure S5: Generation of the KRAS^{G12D} transgenic cell-line in *Killibow*-derived cells

a) The KRAS^{G12D} lentiviral plasmid was generated by replacing the GFP (from the EF-1α-HygR-P2A-GFP plasmid) with the human KRAS^{G12D} sequence.

Acknowledgements

We thank the Harel lab for stimulating discussion and feedback on the manuscript. We thank Yonatan Birnbaum and Fatma Idrees for killifish maintenance, and Naomi Melamed-Book from the imaging facility (HUJI). Supported by the Zuckerman Program (I.H.), ISF 2178/19 (I.H.), Israeli Ministry of Science 3-17631 (I.H.), 3-16872 (I.H.), the Moore Foundation GBMF9341 (I.H.), BSF-NSF 2020611 (I.H.), the Israeli Ministry of Agriculture 12-16-0010 (I.H), and the Levi Eshkol scholarship of the Israeli Ministry of Science (E.M.), Czech Science Foundation (grant number 22-01781O) and Ministry of Education, Youth and Sports of the Czech Republic - project Biodiversity (CZ.02.1.01/0.0/0.0/16_025/0007370) (R.F.).

RESOURCE AVAILABILITY

Data and Code availability

All raw RNA sequencing data, as well as processed datasets could be found in the GEO database, accession number GSE226279. The code is available in the GitHub repository for this paper https://github.com/Harel-lab/Killibow-rag2-mutant.

EXPERIMENTAL MODEL AND SUBJECT DETAILS

African turquoise killifish strain, husbandry, and maintenance

The African turquoise killifish (GRZ strain) were housed as previously described[23,46]. Fish were grown at 28°C in a central filtration recirculating system with a 12 h light/dark cycle at the Hebrew University of Jerusalem (Aquazone ltd, Israel). Fish were fed with live Artemia until the age of 2 weeks (#109448, Primo), and starting week 3, fish were fed three times a day on weekdays (and once a day on weekends), with GEMMA Micro 500 Fish Diet (Skretting Zebrafish, USA), supplemented with Artemia once a day. All turquoise killifish care and uses were approved by the Subcommittee on Research Animal Care at the Hebrew University of Jerusalem (IACUC protocols #NS-18-15397-2 and #NS-22-16915-3).

CRISPR/Cas9 target prediction and gRNA synthesis

CRISPR/Cas9 genome-editing protocols were performed according to[23,46]. In brief, for targeting the *rag2* gene, gRNA target sites were identified using CHOPCHOP (https://chopchop.rc.fas.harvard.edu/)[68], and are shown below. PAM sites are shown in bold,

and when needed, the first base-pair was changed to a 'G' to comply with the T7 promoter. Design of variable oligonucleotides, and hybridization with a universal reverse oligonucleotide was performed according to[23], and the resulting products were used as a template for *in vitro* transcription. gRNAs were *in-vitro* transcribed and purified using TranscriptAid T7 High Yield Transcription Kit (Thermo Scientific #K0441), according to the manufacturer's protocol.

Gene name	gRNA sequence
Rag2 (Exon 1, XM_015964119.1)	GGGAGTTACATCATTCACGGCGG

Production of Cas9 and transposase mRNA

Experiments were performed according to[23,27,46]. The pCS2-nCas9n expression vector was used to produce Cas9 mRNA (Addgene, #47929)[69], and the PCS2FA plasmid was used to produce transposase mRNA[70]. PCS2FA is available from Kawakami, N. (kokawaka@lab.nig.ac.jp). Capped and polyadenylated mRNA was *in-vitro* transcribed and purified using the mMESSAGE mMACHINE SP6 ULTRA (ThermoFisher # AM1340).

Production of Cre mRNA

A Cre-GFP DNA cassette was amplified from pCAG-Cre:GFP (Addgene #13776) using a forward primer (CreF: TGAGCCGCCACCATGGC), and M13 reverse primer (M13R: CAGGAAACAGCTATGAC). SP6 promoter was then added by a second round of amplification using the following forward primer: (SP6F: CCCTAGGTATTTAGGTGACACTATAGTGAGCCGCCACCATGGC). PCR products were sequence verified and purified using standard methods. The clean SP6-Cre-GFP cassette was then used as template for *in-vitro* RNA transcription. Capped and polyadenylated mRNA was *in-vitro* transcribed and purified using the mMESSAGE mMACHINE SP6 ULTRA (ThermoFisher # AM1340).

Microinjection of turquoise killifish embryos

For generation of *rag2* mutant fish using CRISPR/Cas9, microinjection of turquoise killifish embryos was performed according to[23]. Briefly, nCas9n-encoding mRNA (300 ng/µL) and gRNA (30 ng/µL) were mixed with phenol-red (P0290, Sigma-Aldrich) and co-injected into two-cell stage fish embryos. Sanger DNA sequencing was used for detecting successful germline transmission on F1 embryos using the following primer sequences: rag2F: TGATGTTTTCTGTTTTGACCCA and rag2R: TATCTGTGGGCAGGACCTGTA. Fish with

desired alleles were further outcrossed to minimize potential off-target effects, and maintained as stable lines. For generation of transgenic *Killibow* fish using Tol2, transposase-encoding mRNA (300 ng/µL) and the *Zebrabow* vector (30 ng/µL, Addgene #118219) were co-injected into one-cell stage fish embryos as described above. Successful germline transmission on F1, and selection of founders was performed according to the uniformity and intensity of the RFP signal.

Estimation of transgene copy number in the *Killibow*

In order to estimate the copy number of the *Killibow* transgene in the killifish genome we performed real time qPCR on genomic DNA (gDNA) extracted from cultured fibroblasts form *Killibow* fish. gDNA was extracted using a standard gDNA extraction kit (QIAGEN #56304) according to the manufacturer instructions. Next, we performed a pPCR to compare between a reference gene, 16S ribosomal RNA (16S-F: AGCCTCGCCTGTTTACCAAA, 16S-R: TTGCACGGTCAAAATACCGC), and the *Killibow* transgenic construct[13] (Killi-F: TTCATGTACGGCTCCAAGGC, Killi-R: ACCTTGTAGATCAGCGTGCC). To further explore whether amplification is affected by gDNA concentration, we conducted the qPCR using various concentrations by diluting *Killibow* gDNA in WT gDNA. Copy number was determined using the comparative Ct method ($2^{-(\Delta\Delta cq)}$)[71]. Our qPCR data demonstrated that there is a liner correlation between the amount of *Killibow* gDNA and amplification cycle, with a ~70-fold difference between our reference gene and the *Killibow* construct.

METHOD DETAILS

Tail regeneration

Regeneration protocols were adapted from[45]. Briefly, one-month or four-month-old fish were sedated in MS222 (200 mg/L), placed on a damp kimwipe, and approximately 50% of their tail was amputated using a square razor in one clean cut. Pictures were taken using a Leica MC190HD camera mounted on a Leica M165FC microscope before and after amputation, and every 3 days for 18 days.

Generation of the *Killibow* cell-line

Cells were isolated as described previously[46]. Briefly, adult fish were sedated with MS-222 (200 mg/L Tricaine, and a 2–3 mm tissue was trimmed from the tail fin using a sterile razor blade. Following disinfection, tissue samples were incubated for 2 h with 1 mL of an antibiotic

solution containing Gentamicin (50 µg/mL Gibco) and Primocin™ (50 µg/mL, InvivoGen) in DPBS at room temperature. Tissues were then transferred into an enzymatic digestion buffer (200 µL, in a 24-well plate) containing Dispase II (2 mg/mL, Sigma Aldrich) and Collagenase Type P (0.4 mg/mL, Merck Millipore) in Leibovitz's L-15 Medium (Gibco), and mechanical dissociation was applied with a sterile pair of scissors. Crudely dissociated tissue was incubated in the enzymatic digestion buffer for 15 min. The digested tissue was then mixed with 400 µL of complete Leibovitz's L-15 growth medium (Gibco), supplemented with Fetal Bovine Serum (15% FBS, Gibco), penicillin/streptomycin (50 U/ml, Gibco), Gentamicin (Gibco, 50 µg/ml) and Primocin™ (50 µg/ml, InvivoGen). On the following day, media was carefully replaced, and during the first 7 days, cells were daily washed with fresh media before adding new media. When cells reached 85–90% confluency, they were passaged with Trypsin-EDTA 0.05% (0.25% Trypsin-EDTA, diluted in DPBS). Cells were incubated at 28°C humidified incubator (Binder, Thermo Scientific) with normal air composition, and were passaged for ~20 passages.

Plasmid transfection and tamoxifen treatment

Killibow cells were transfected with pCAG-ERT2-Cre-ERT2 plasmid (Addgene #13777, and a Tol2-ubi-ERT2-Cre-ERT2 construct, a kind gift from Wang Wei) using Optim-MEM according to manufacturing protocol. 48 hours post transfection 5-10µM 4-hydroxytamoxifen (Sigma, #H7904-5MG) was added for 24 h, and then washed with fresh media. Cells were imaged ~10 days after treatment.

Plasmid electroporation

Electroporation was performed as previously described[43]. Briefly, 5 µl of a solution containing a Cre-GFP plasmid (~2 µg/µl, Addgene #13776) and phenol red (0.1% Sigma #P0290) was injected intramuscularly using a Nanofil syringe (WPI, #NANOFIL). Fish were then electroporated using 7 mm tweezer electrodes (NEP GENE #CUY650P10) with the ECM 830 generator. (BTX #45-0661). Electrodes were coated with wet cotton to minimize the risk to the fish. Fish were electroporated with 6 pulses of 28 V, for 60 ms each with an interval of 1 s between each pulse. Images were recorded by a Leica MC190HD camera mounted on a Leica M156FC microscope.

Cell transplantation

The *Killibow* cell-line, described above, was injected into either WT or *rag2* homozygous fish (40,000 cells/µl, at 4 µl per fish). Recipient fish were anesthetized adult males (~1.5-

month-old), and intramuscular injection was performed using a Nanofil syringe (WPI, #NANOFIL).

Lentivirus Production and transduction

We synthesized the killifish *kras* gene with the *kras*^{G12D} mutation[39] using gblocks gene synthesis (IDT), and used Gibson assembly to clone it into a lentiviral vector (#99375, Addgene, containing a hygromycin resistance marker). Viruses were produced according to standard procedures using commercially available plasmids (pMD2.G Addgene #12259, psPAX Addgene #12260). Briefly, HEK293T cells were plated at a density ~60,000 cells/cm^2 in DMEM (Invitrogen) supplemented with penicillin/streptomycin/glutamine (Invitrogen), and 10% fetal bovine serum. HEK293T were transfected according to standard procedures. After 24 h, plates were rinsed with 1X PBS and media was replaced. Media containing virus was collected 48 h post transfection, and used for transduction. Finally, transduced *Killibow* cells were grown with media containing Hygromycin (200µg/ml) for selection.

Fluorescence microscopy

Organs were dissected on ice, and imaged using a fluorescent binocular stereo microscope (Leica S9E). Cells were plated on a µ-Slide 8 Well Glass Bottom plates (ibidi, #80827). Imaging was performed on live cells, either using a laser scanning confocal microscope (FV-1200, Olympus, Japan), or a fully motorized Olympus IX23 microscope with an Olympus DP28 camera.

RNA-seq library preparation

Head kidney was isolated as described in[23]. Samples were disrupted by bead beating in 300 µl of TriZol (Sigma) and a single 3 mm metal bead (Eldan, BL6693003000) using TissueLyzer LT (QIAGEN, #85600) with a dedicated adaptor (QIAGEN, #69980). Beating was performed at 50 Hz for 5 min. RNA extraction was performed with TRI Reagent (Sigma, #T9424) RNA concentration and quality were determined by using an Agilent 2100 bioanalyser (Agilent Technologies). Library preparation was performed using KAPA mRNA HyperPrep Kit (ROCHE-08105936001) according to the recommended protocols. Library quantity and pooling were measured by Qubit (dsDNA HS, Q32854), Size selection at 4% agarose gel. Library quality was measured by Tape Station (HS, 5067-5584). Libraries were sequenced by NextSeq 2000 P2, 100 cycle,75 bp single-end (Illumina, 20024906) with ~40 million reads per sample.

RNA sequencing analysis

Quality control and adapter trimming of the fastq sequence files were performed with FastQC (v0.11.8)[72], fastx-toolkits (v0.0.13), Trim Galore! (v0.6.4) [73], and Cutadapt (3.4) [74]. Options were set to remove Illumina TruSeq adapters and end sequences to retain high-quality bases with *phred* score > 20 and a remaining length > 20 bp. Successful processing was verified by re-running FastQC. Reads was mapped and quantified to the killifish genome Nfu_20140520 [29,30] using STAR 2.7.6a[75]. Differential gene expression between *rag2* mutant and WT fish was performed using the edgeR package (v3.32.1)[76,77].

Gene Ontology Enrichment Analysis

Enriched Gene Ontology (GO) terms associated with transcripts level was identified using GO implemented in R package clusterProfiler (v3.18.1)[78] with the threshold of p-value (uncorrected) < 0.05 and log2(FC) > 1. GO terms were based on human GO annotations from org.Hs.eg.db (v3.13.0) [79] and AnnotationDbi (v1.54.1)[80].

References:

1. Radtke, F. & Clevers, H. Self-renewal and cancer of the gut: two sides of a coin. *Science (80-.).* **307**, 1904–1909 (2005).

2. Rossi, D. J., Jamieson, C. H. M. & Weissman, I. L. Stems cells and the pathways to aging and cancer. *Cell* **132**, 681–696 (2008).

3. Sharpless, N. E. & DePinho, R. A. How stem cells age and why this makes us grow old. *Nat. Rev. Mol. cell Biol.* **8**, 703–713 (2007).

4. López-Otín, C., Blasco, M. A., Partridge, L., Serrano, M. & Kroemer, G. The hallmarks of aging. *Cell* **153**, 1194–1217 (2013).

5. Niccoli, T. & Partridge, L. Ageing as a risk factor for disease. *Curr Biol* **22**, R741-52 (2012).

6. Lawson, D. A., Kessenbrock, K., Davis, R. T., Pervolarakis, N. & Werb, Z. Tumour heterogeneity and metastasis at single-cell resolution. *Nat. Cell Biol.* **20**, 1349–1360 (2018).

7. Jackson, H. W. *et al.* The single-cell pathology landscape of breast cancer. *Nature* **578**, 615–620 (2020).

8. Kinker, G. S. *et al.* Pan-cancer single-cell RNA-seq identifies recurring programs of cellular heterogeneity. *Nat. Genet.* **52**, 1208–1218 (2020).

9. Hernandez-Segura, A. *et al.* Unmasking transcriptional heterogeneity in senescent cells. *Curr. Biol.* **27**, 2652–2660 (2017).

10. Cohn, R. L., Gasek, N. S., Kuchel, G. A. & Xu, M. The heterogeneity of cellular senescence: insights at the single-cell level. *Trends Cell Biol.* (2022).

11. Kimmel, J. C. *et al.* Murine single-cell RNA-seq reveals cell-identity-and tissue-specific trajectories of aging. *Genome Res.* **29**, 2088–2103 (2019).

12. Consortium, T. M., h, O. coordination S. N. 1 K. J. 2 N. N. F. 2 M. A. P. 2 Q. S. R. quake@ stanford. edu 2 3 f W.-C. T. twc@ stanford. edu 4 5 6 g D. S. spyros. darmanis@ czbiohub. org 2, 3, L. coordination B. J. 2 B. O. 2 C. M. B. 3 C. S. 2 G. F. 2 J. R. C. 3 M. A. 2 P. L. 2 P. A. O. 2 S. R. V. 2 S. G. M. 3 W. J. T. 2 Z. F. & 3, C. data analysis B. J. 2 B. O. 2 C. P. 2 C. D. 3 D. S. 2 D. J. L. 2 27 K. J. 2 P. A. O. 2 S. G. M. 3 W. J. T. 2 Z. F. Single-cell transcriptomics of 20 mouse organs creates a Tabula

Muris. *Nature* **562**, 367–372 (2018).

13. Pan, Y. A. *et al.* Zebrabow: multispectral cell labeling for cell tracing and lineage analysis in zebrafish. *Development* **140**, 2835–2846 (2013).

14. Wagner, D. E. & Klein, A. M. Lineage tracing meets single-cell omics: opportunities and challenges. *Nat. Rev. Genet.* **21**, 410–427 (2020).

15. Baron, C. S. & van Oudenaarden, A. Unravelling cellular relationships during development and regeneration using genetic lineage tracing. *Nat. Rev. Mol. cell Biol.* **20**, 753–765 (2019).

16. VanHorn, S. & Morris, S. A. Next-generation lineage tracing and fate mapping to interrogate development. *Dev. Cell* **56**, 7–21 (2021).

17. Jordan, C. T., Guzman, M. L. & Noble, M. Cancer stem cells. *N. Engl. J. Med.* **355**, 1253–1261 (2006).

18. Reya, T., Morrison, S. J., Clarke, M. F. & Weissman, I. L. Stem cells, cancer, and cancer stem cells. *Nature* **414**, 105–111 (2001).

19. Fane, M. & Weeraratna, A. T. How the ageing microenvironment influences tumour progression. *Nat. Rev. Cancer* **20**, 89–106 (2020).

20. Harel, I. & Brunet, A. The African Turquoise Killifish: A Model for Exploring Vertebrate Aging and Diseases in the Fast Lane. *Cold Spring Harb Symp Quant Biol* (2015) doi:10.1101/sqb.2015.80.027524.

21. Kim, Y., Nam, H. G. & Valenzano, D. R. The short-lived African turquoise killifish: an emerging experimental model for ageing. *Dis Model Mech* **9**, 115–129 (2016).

22. Cellerino, A., Valenzano, D. R. & Reichard, M. From the bush to the bench: the annual Nothobranchius fishes as a new model system in biology. *Biol Rev Camb Philos Soc* (2015) doi:10.1111/brv.12183.

23. Astre, G., Moses, E. & Harel, I. The African turquoise killifish (Nothobranchius furzeri): biology and research applications. in *Laboratory Fish in Biomedical Research* 245–287 (Elsevier, 2022).

24. Harel, I. The turquoise killifish. *Nat. Methods* (2022) doi:10.1038/s41592-022-01631-y.

25. Platzer, M. & Englert, C. Nothobranchius furzeri: A Model for Aging Research and

More. *Trends Genet* **32**, 543–552 (2016).

26. Harel, I. *et al.* A platform for rapid exploration of aging and diseases in a naturally short-lived vertebrate. *Cell* (2015) doi:10.1016/j.cell.2015.01.038.

27. Harel, I., Valenzano, D. R. & Brunet, A. Efficient genome engineering approaches for the short-lived African turquoise killifish. *Nat. Protoc.* (2016) doi:10.1038/nprot.2016.103.

28. Cui, R. *et al.* Relaxed Selection Limits Lifespan by Increasing Mutation Load. *Cell* **178**, 385-399 e20 (2019).

29. Valenzano, D. R. *et al.* The African Turquoise Killifish Genome Provides Insights into Evolution and Genetic Architecture of Lifespan. *Cell* **163**, 1539–1554 (2015).

30. Reichwald, K. *et al.* Insights into Sex Chromosome Evolution and Aging from the Genome of a Short-Lived Fish. *Cell* **163**, 1527–1538 (2015).

31. Couëdel, C. *et al.* Analysis of mutations from SCID and Omenn syndrome patients reveals the central role of the Rag2 PHD domain in regulating V (D) J recombination. *J. Clin. Invest.* **120**, 1337–1344 (2010).

32. Villa, A. *et al.* V (D) J recombination defects in lymphocytes due to RAG mutations: severe immunodeficiency with a spectrum of clinical presentations. *Blood, J. Am. Soc. Hematol.* **97**, 81–88 (2001).

33. Tang, Q. *et al.* Optimized cell transplantation using adult rag2 mutant zebrafish. *Nat. Methods* **11**, 821–824 (2014).

34. Bradshaw, W. J., Poeschla, M., Placzek, A., Kean, S. & Valenzano, D. R. Extensive age-dependent loss of antibody diversity in naturally short-lived turquoise killifish. *Elife* **11**, (2022).

35. Press, C. M. & Evensen, Ø. The morphology of the immune system in teleost fishes. *Fish Shellfish Immunol.* **9**, 309–318 (1999).

36. Casey, M. J. & Stewart, R. A. Pediatric cancer models in zebrafish. *Trends in cancer* **6**, 407–418 (2020).

37. Ju, B. *et al.* Oncogenic KRAS promotes malignant brain tumors in zebrafish. *Mol. Cancer* **14**, 1–11 (2015).

38. Nguyen, A. T. *et al.* An inducible kras V12 transgenic zebrafish model for liver

tumorigenesis and chemical drug screening. *Dis. Model. Mech.* **5**, 63–72 (2012).

39. Langenau, D. M. *et al.* Effects of RAS on the genesis of embryonal rhabdomyosarcoma. *Genes Dev.* **21**, 1382–1395 (2007).

40. Livet, J. *et al.* Transgenic strategies for combinatorial expression of fluorescent proteins in the nervous system. *Nature* **450**, 56–62 (2007).

41. Mosimann, C. *et al.* Ubiquitous transgene expression and Cre-based recombination driven by the ubiquitin promoter in zebrafish. *Development* **138**, 169–177 (2011).

42. Gupta, V. & Poss, K. D. Clonally dominant cardiomyocytes direct heart morphogenesis. *Nature* **484**, 479–484 (2012).

43. Moses, E. & Harel, I. A scalable platform for functional interrogation of peptide hormones in fish. *bioRxiv* 2001–2023 (2023).

44. Lopez-Otin, C., Blasco, M. A., Partridge, L., Serrano, M. & Kroemer, G. The hallmarks of aging. *Cell* **153**, 1194–1217 (2013).

45. Wendler, S., Hartmann, N., Hoppe, B. & Englert, C. Age-dependent decline in fin regenerative capacity in the short-lived fish Nothobranchius furzeri. *Aging Cell* **14**, 857–866 (2015).

46. Astre, G. *et al.* Sex-specific regulation of metabolic health and vertebrate lifespan by AMP biosynthesis. *bioRxiv* 2022.01.10.475524 (2022) doi:10.1101/2022.01.10.475524.

47. Indra, A. K. *et al.* Temporally-controlled site-specific mutagenesis in the basal layer of the epidermis: comparison of the recombinase activity of the tamoxifen-inducible Cre-ERT and Cre-ERT2 recombinases. *Nucleic Acids Res.* **27**, 4324–4327 (1999).

48. Metzger, D., Clifford, J., Chiba, H. & Chambon, P. Conditional site-specific recombination in mammalian cells using a ligand-dependent chimeric Cre recombinase. *Proc. Natl. Acad. Sci.* **92**, 6991–6995 (1995).

49. Hao, Z. & Rajewsky, K. Homeostasis of peripheral B cells in the absence of B cell influx from the bone marrow. *J. Exp. Med.* **194**, 1151–1164 (2001).

50. Cannon, J. P. *et al.* A bony fish immunological receptor of the NITR multigene family mediates allogeneic recognition. *Immunity* **29**, 228–237 (2008).

51. Yoder, J. A. Form, function and phylogenetics of NITRs in bony fish. *Dev. Comp.*

Immunol. **33**, 135–144 (2009).

52. Renshaw, S. A. & Trede, N. S. A model 450 million years in the making: zebrafish and vertebrate immunity. *Dis Model Mech* **5**, 38–47 (2012).

53. Moore, F. E. *et al.* Single-cell transcriptional analysis of normal, aberrant, and malignant hematopoiesis in zebrafish. *J. Exp. Med.* **213**, 979–992 (2016).

54. Carmona, S. J. *et al.* Single-cell transcriptome analysis of fish immune cells provides insight into the evolution of vertebrate immune cell types. *Genome Res.* **27**, 451–461 (2017).

55. Pereiro, P. *et al.* Zebrafish Nk-lysins: first insights about their cellular and functional diversification. *Dev. Comp. Immunol.* **51**, 148–159 (2015).

56. Dornburg, A. & Yoder, J. A. On the relationship between extant innate immune receptors and the evolutionary origins of jawed vertebrate adaptive immunity. *Immunogenetics* 1–18 (2022).

57. Yoder, J. A. *et al.* Resolution of the novel immune-type receptor gene cluster in zebrafish. *Proc. Natl. Acad. Sci.* **101**, 15706–15711 (2004).

58. Tacutu, R. *et al.* Human Ageing Genomic Resources: new and updated databases. *Nucleic Acids Res* **46**, D1083–D1090 (2018).

59. Schartl, M. Beyond the zebrafish: diverse fish species for modeling human disease. *Dis Model Mech* **7**, 181–192 (2014).

60. Podrabsky, J. E., Riggs, C. L. & Wagner, J. T. Tolerance of Environmental Stress. in *Annual Fishes. Life History Strategy, Diversity, and Evolution* (eds. Berois, N., García, G. & De Sá, R. O.) 159–184 (CRC Press, Taylor & Francis, 2016). doi:10.1201/b19016.

61. Jaggard, J. B. *et al.* Cavefish brain atlases reveal functional and anatomical convergence across independently evolved populations. *Sci. Adv.* **6**, eaba3126 (2020).

62. Wang, W. *et al.* Changes in regeneration-responsive enhancers shape regenerative capacities in vertebrates. *Science (80-.).* **369**, (2020).

63. Batlle, E. & Clevers, H. Cancer stem cells revisited. *Nat. Med.* **23**, 1124–1134 (2017).

64. Krug, J. *et al.* Generation of a transparent killifish line through multiplex CRISPR/Cas9mediated gene inactivation. *Elife* **12**, e81549 (2023).

65. Rozenberg, I., Moses, E. & Harel, I. CRISPR–Cas9 Genome Editing in Nothobranchius furzeri for Gene Knockout and Knock-In. *Cold Spring Harb. Protoc.* (2022).

66. Oginuma, M. *et al.* Rapid reverse genetics systems for Nothobranchius furzeri, a suitable model organism to study vertebrate aging. *Sci. Rep.* **12**, 11628 (2022).

67. Nath, R. D., Bedbrook, C. N., Nagvekar, R., Deisseroth, K. & Brunet, A. Rapid and precise genome engineering in a naturally short-lived vertebrate. *bioRxiv* 2005–2022 (2022).

68. Labun, K. *et al.* CHOPCHOP v3: expanding the CRISPR web toolbox beyond genome editing. *Nucleic Acids Res.* **47**, W171–W174 (2019).

69. Jao, L. E., Wente, S. R. & Chen, W. Efficient multiplex biallelic zebrafish genome editing using a CRISPR nuclease system. *Proc Natl Acad Sci U S A* **110**, 13904–13909 (2013).

70. Kawakami, K., Shima, A. & Kawakami, N. Identification of a functional transposase of the Tol2 element, an Ac-like element from the Japanese medaka fish, and its transposition in the zebrafish germ lineage. *Proc Natl Acad Sci U S A* **97**, 11403–11408 (2000).

71. Livak, K. J. & Schmittgen, T. D. Analysis of relative gene expression data using real-time quantitative PCR and the $2^{-\Delta\Delta CT}$ method. *methods* **25**, 402–408 (2001).

72. Andrews, S. FastQC: a quality control tool for high throughput sequence data. 2010. (2017).

73. Krueger, F. Trim galore. *A wrapper tool around Cutadapt FastQC to consistently apply Qual. Adapt. trimming to FastQ files* **516**, 517 (2015).

74. Martin, M. Cutadapt removes adapter sequences from high-throughput sequencing reads. *EMBnet. J.* **17**, 10–12 (2011).

75. Dobin, A. *et al.* STAR: ultrafast universal RNA-seq aligner. *Bioinformatics* **29**, 15–21 (2013).

76. McCarthy, D. J., Chen, Y. & Smyth, G. K. Differential expression analysis of multifactor RNA-Seq experiments with respect to biological variation. *Nucleic Acids Res.* **40**, 4288–4297 (2012).

77. Robinson, M. D., McCarthy, D. J. & Smyth, G. K. edgeR: a Bioconductor package for differential expression analysis of digital gene expression data. *Bioinformatics* **26**, 139–140 (2010).

78. Yu, G., Wang, L.-G., Han, Y. & He, Q.-Y. clusterProfiler: an R package for comparing biological themes among gene clusters. *Omi. a J. Integr. Biol.* **16**, 284–287 (2012).

79. Carlson, M., Falcon, S., Pages, H. & Li, N. org. Hs. eg. db: Genome wide annotation for Human. *R Packag. version* **3**, (2019).

80. Pagès, H., Carlson, M., Falcon, S. & Li, N. AnnotationDbi: Manipulation of SQLite-based annotations in Bioconductor. R package version1. 54.1. (2021).